A GIC Estimator for Electric Grid Monitoring During Geomagnetic Disturbances

Cecilia Klauber, *Student Member, IEEE*, Komal Shetye, *Senior Member, IEEE*, Thomas J. Overbye, *Fellow, IEEE*, Katherine Davis, *Senior Member, IEEE*

***Abstract*—Electric power system state estimation is a vital part of real-time monitoring and management for power grid operations and control. With increased interest in the effects of geomagnetically induced currents (GICs) and effective mitigation strategies therein, similar tools that provide situational awareness during GMD events are increasingly necessary. Therefore, a GIC estimator is developed by relating the known system parameters and measurements to the current "GIC state," from which the GIC currents in transformers can be quickly calculated. Due to the linearity of GIC relationships, the estimator solves quickly and efficiently. The proposed methods are tested on a small example and a synthetic Texas 2000 bus scenario. These studies show the effectiveness of a GIC estimator to provide situational awareness for real-time operations, as well as sensitivity to measurement uncertainty and availability.**

***Index Terms*—geomagnetic disturbance (GMD), geomagnetically induced currents (GICs), state estimation**

I. Introduction

Geomagnetic disturbances (GMDs) such as coronal mass ejections and solar storms cause disturbances in earth's magnetic field. These geomagnetic field variations induce low frequency (quasi-dc, less than 0.1 Hz) electric fields on the earth. Geomagnetically induced currents (GICs) are produced by these fields and flow in the earth and high voltage transmission lines, due to the lines' low dc resistance [1].

From a power systems perspective, GICs cause half cycle saturation of transformers and consequently affect the power grid with harmonics and reactive power losses [2], [3]. The heating of transformers can lead to transformer damage and the reactive power losses contribute to suboptimal voltage profile and even voltage collapse [4], [5]. These issues are the source of concern for power system operators and planners. The potential of GMDs to impact power grid operation has been known for decades and is receiving increased recognition as the North American Electric Reliability Corporation (NERC) has mandated vulnerability assessments and mitigation plans from industry [6]. In efforts to understand and mitigate these impacts, improved GIC modeling and monitoring is being pursued in academia and industry, see [7]–[13]. Regarding mitigation, short-term operational strategies rely on real-time visibility of the current system state with respect to GICs [14], [15], while long-term techniques still require accurate modeling and some measurement availability [16]. Beyond [17], [18], few accounts of tools for real-time GMD monitoring and management exist.

State estimation (SE) for transmission systems is a fundamental tool, enabling nearly real-time system state awareness through established techniques for processing measurement and topology data. The availability and accuracy of this base state is invaluable for system management, providing key inputs for a variety of system security and control methods [19]–[21]. Previous work [22] demonstrated the estimation error incurred by not incorporating GIC-related measurements and models in the standard SE formulation during a GMD. The purpose of the present work, though, is to take a first step toward integrated and improved monitoring by formulating and testing an SE-type method for GIC real-time system awareness. This GIC estimator can provide widespread visibility into GMD-induced system behavior, supplying the data for visualization of GIC flows and reactive power losses. The resulting estimates can also be used to provide vital inputs for operational schemes, such as mitigation strategies which rely on effective GIC information to leverage line switching, generation redispatch, and general reactive power support [14], [15], [23], [24]. Estimated transformer reactive power losses could be integrated with a standard SE to improve traditional voltage state estimates despite lack of integrated GIC modeling.

There is currently a general lack of measurement devices installed on the electric power grid to meter GMD-related quantities. In practice, only a fraction of transformers are equipped with GIC neutral current monitors and magnetometer data is sparse as well. Rather than be measured directly, the key input of electric field values is often estimated from magnetic field (magnetometer) measurements and earth conductivity profiles. Because of regulatory requirements, proliferation of metering devices is likely to increase as real-time visibility of network GIC flows will likely play a role in many preparedness plans. Similar to how traditional SE is used to clean and consolidate data for use in other processes, comparable techniques for GMD-related values may soon find wide application among power system operators as metering increases and as new tools which rely on advanced metering motivate yet additional installations.

The contribution of this work is the development and testing of a quick and versatile GIC estimation methodology. While

This work is funded by the National Science Foundation under grant "EAR-1520864: Hazards SEES: Improved prediction of geomagnetic disturbances, geomagnetically induced currents, and their impacts on power distribution systems." The authors would also like to thank Jennifer Gannon of Computational Physics, Inc. for usage of her figure and input.

The authors are with the Department of Electrical and Computer Engineering, Texas A&M University, College Station, TX, USA;
(email: cklauber,shetye,overbye,katedavis@tamu.edu)

Accepted for publication in IEEE Transactions on Power Systems, June 2020

there are a number of real-time GIC simulators covered in the literature [25], the proposed estimator provides a more accurate and complete snapshot of the GICs flowing through the system by leveraging all available measurements in real-time. Other research related to GIC estimation and monitoring is either not intended for real-time usage [26], [27] or assumes a uniform electric field. For example, in [17] a uniform magnetic field was assumed, as data was only available from one magnetometer. The present work considers a non-uniform response mapped to pre-defined electric field zones. This design is inspired by recent magnetometer installations, such as that in the state of Texas, and enables improved accuracy due to the finer granularity of the resulting estimates.

The remainder of the paper is organized as follows: Section II details the modeling of GICs using dc analysis. Section III presents a brief overview of traditional SE methods and the development of the GIC estimation framework. A small example is also included. Section IV demonstrates the proposed techniques using the synthetic Texas 2000 bus case, including exploration of method reliability under measurement uncertainty and varying availability. Areas for future work and conclusions are presented in Section V.

II. GIC Modeling

Modeling of GIC effects on power systems has been described in [1], [3] and is summarized in this section in preparation for the proposed GIC estimation formulation. To calculate the GICs flowing in the system, first the induced voltage potential on a transmission line is found by integrating the electric field over the length of the line. For a uniform electric field, the (dc) voltage on the line between buses n and m is modeled as

$$V_{nm} = E^N L^N_{nm} + E^E L^E_{nm} \tag{1}$$

where E^N and E^E are the northward and eastward components of the electric field vector and L^N_{nm} and L^E_{nm} are the northward and eastward distances of the line between buses n and m, as described in [28]. The induced voltages are converted to dc current injections by Norton's Equivalent and the total current injection can then be found via Kirchhoff's current law. The resulting vector is given by $\mathbf{I} = \mathbf{HE}$, where $\mathbf{H}$ depends on the length, resistance, and orientation of the lines. For a uniform electric field, $\mathbf{E} \in \mathbb{R}^{2\times 1}$ and $\mathbf{H} \in \mathbb{R}^{(n_b+n_s)\times 2}$, where n_b and n_s are the number of buses and substations in the system, respectively. For a non-uniform electric field, the system can be divided into k predetermined electric field zones, which could each be experiencing a different electric field. The granularity and boundaries of these electric field zones can be determined based on regional conductivity, available metering, and/or expected electric field variation. Expected variation depends on the storm and earth models, but studies have shown that electric field differences across geographic distances of 200 km can differ by up to two orders of magnitude [29]. Non-uniform electric fields necessitate the creation of a vector $\mathbf{E} \in \mathbb{R}^{2k\times 1}$ of the electric field components. Correspondingly, the distance components L^N_{nm} and L^E_{nm} are separated to represent the portion of the line in each zone. However, $\mathbf{H} \in \mathbb{R}^{(n_b+n_s)\times 2k}$ will still be quite sparse as the voltage induced on a line between two buses usually depends on at most a few electric fields. The dc line voltage calculation of Eq. 1 is now the summation of up to $2k$ terms. Furthermore, a disturbance with non-linear magnitude and uniform direction could be considered, in which case $\mathbf{E}$ would have length $k+1$, i.e., k magnitudes and one direction. Whether uniform or non-uniform electric fields are used, the dc voltage (V_n) at a bus or substation neutral is determined by solving the dc network

$$\mathbf{V} = \mathbf{G}^{-1}\mathbf{I} = \mathbf{G}^{-1}\mathbf{HE} \tag{2}$$

where $\mathbf{G} \in \mathbb{R}^{(n_b+n_s)\times(n_b+n_s)}$ is a square matrix of line conductance values augmented to include substation grounding resistances values.

The GIC flows from node n to node m are determined by

$$I_{nm} = g_{nm}(V_n - V_m) \tag{3}$$

where g_{nm} is the connecting line conductance from $\mathbf{G}$. The effective GIC, $\mathcal{I}_t$, is the effective per phase current depending on transformer t's type and configuration. For simple cases, such as for GSU transformers, $\mathcal{I}_t$ is merely the current in the grounded (high-side) winding. Otherwise $\mathcal{I}_t$ depends on the current in both coils [3]. According to [9],

$$\mathcal{I}_t = \left| I_{H,t} + \frac{I_{L,t}}{a_t} \right| \tag{4}$$

where $I_{H,t}$ is the per phase GIC going into the high side winding, the series winding for an autotransformer, $I_{L,t}$ is the per phase GIC going into the low side of the transformer, and a_t is the transformer turns ratio. In matrix form, (4) for all transformers is given by

$$\boldsymbol{\mathcal{I}} = \left| \mathbf{\Phi G}^{-1}\mathbf{HE} \right| \tag{5}$$

where $\mathbf{\Phi}$ is a sparse matrix with entries consisting of substation and transformer conductances. GIC flows through a transformer effectively increase its reactive power losses linearly with the respect to the effective GICs. The additional reactive power loss in Mvar is given by

$$Q_{loss,t} = k_t V_{pu,t} \mathcal{I}_t \tag{6}$$

where $V_{pu,t}$ is the per unit ac terminal voltage for transformer t, and k_t is a scalar specific to the transformer. These losses due to the GICs in the dc network affect the ac network by drawing additional reactive power and generally lowering the system voltage profile.

It is also useful to define the relationship between transformer neutral currents, which are sparsely metered, and the driving electric fields. Let $\boldsymbol{\mathcal{I}}_n$ be the vector of all n_t transformer neutral GIC currents and $\mathbf{\Phi}_n \in \mathbb{R}^{n_t\times(n_b+n_s)}$ be also a sparse matrix with transformer conductance entries, then

$$\boldsymbol{\mathcal{I}}_n = \mathbf{\Phi}_n \mathbf{G}^{-1}\mathbf{HE}. \tag{7}$$

Leveraging modeling of the dc network for monitoring purposes will enable previously unavailable insight which can assist grid operators during geomagnetic disturbances.

III. State Estimation and Formulation

A. Traditional State Estimation Models

Traditional SE programs utilize system measurements and topology to provide awareness for real-time monitoring. Typical frameworks are formulated as overdetermined systems of nonlinear equations and solved as weighted least squares (WLS) problems [20]. A model relating the states $\mathbf{x}$ to measurement z_i is given by

$$z_i = h_i(\mathbf{x}) + e_i. \tag{8}$$

The relationship between the ith measurement and the states $\mathbf{x}$ is modeled by the function $h_i(\cdot)$, which is nonlinear and non-convex, while e_i is the measurement error, assumed to be normal with zero mean and variance σ_i^2. WLS SE is set up as a quadratic optimization problem with equality/inequality constraints which will minimize the weighted total of the squares of the measurement residuals. More accurate measurements are given more weight and under certain assumptions WLS is also the maximum likelihood method. For power system SE, the problem is solved by iterative methods, due to the nonlinearity of the power flow equations.

B. GIC Estimation Model

A process independent of traditional SE, GIC estimation involves leveraging GIC-related measurements and GIC relationship linearity to estimate distinct GIC states. Complex nodal voltages are neither a measurement nor state, but it should be noted that GIC-derived values (i.e., transformer reactive power losses) could be used to improve the estimation of the typical SE states in post-processing. Other linear estimators have been introduced in part thanks to increasing installations of phasor measurement units [30]–[32]. For GIC estimation, the linear relationship of (7) also enables a linear estimator with similar benefits such as an iterative-free solution. The states shall be the underlying electric field, **E**, specifically the northward and eastward components of each predetermined electric field zone. Analogous to the traditional SE, with this knowledge and an understanding of the system topology one can calculate all other values of interest pertaining to the system, namely effective GICs, reactive power losses, and transformer heating models. The measurement set may include GIC neutral currents from transformers. Regional electric field, **E**, estimates from magnetic field, **B**, measurements shall also be available, as illustrated by $\mathbf{E}_{meas}$ in Fig. 1. Depending on the granularity of available magnetometer measurements and calculated **E** therein, gaps in input **E** are provided via interpolation [33], [34]. The **B** to **E** conversion uses ground conductivity models to covert magnetic field data to electric field data. The present models are derived from magnetotelluric study results and geological data and are available from the United State Geological Survey [35]. Here it will be assumed that the ground model is known such that a **B** measurement can be mapped to an **E** measurement prior to integration with the GIC estimator. The diagram also shows how the resulting states provide valuable inputs for GIC calculators or potential visualization and control tools. Eq. (8)

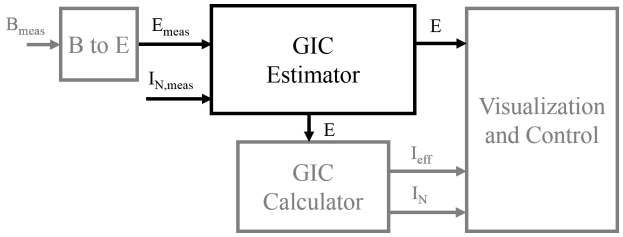

Fig. 1. GIC estimation in the context of a broader GMD monitoring and mitigation scheme for power grid operations

in matrix form for GIC estimation is given by

$$\mathbf{z} = \mathbf{h}\mathbf{x} + \mathbf{e} \tag{9}$$

where

$$\mathbf{h} = \begin{bmatrix} \mathbf{I}_{j\times 2k} \\ \{\mathbf{\Phi}\mathbf{G}^{-1}\mathbf{H}\}_l \end{bmatrix} \tag{10}$$

and $\mathbf{z}$, $\mathbf{x}$, and $\mathbf{e}$ are the vector forms of the measurements, states, and expected noise, respectively. The identity matrix $\mathbf{I}$ has length corresponding to the number of measured states, j, and width equal to two times the number of electric field zones, or the length of $\mathbf{E}$, $2k$. The l rows of $\{\mathbf{\Phi}\mathbf{G}^{-1}\mathbf{H}\}$ correspond to the available $\mathcal{I}_n$ measurements. The resulting linear least squares state estimation optimization problem is as follows:

$$\min \quad (\mathbf{z} - \mathbf{h}\mathbf{x})^T \mathbf{R}^{-1} (\mathbf{z} - \mathbf{h}\mathbf{x}) \tag{11}$$

where $\mathbf{R}$ is the measurement error covariance matrix. The weight matrix, $\mathbf{R}^{-1}$, has diagonal elements $R_i^{-1} = 1/\sigma_i^2$. Due to the linear nature of GIC systems, an analytical solution exists without need for iterating,

$$\mathbf{x} = [\mathbf{h}^T \mathbf{R}^{-1} \mathbf{h}]^{-1} \mathbf{h}^T \mathbf{R}^{-1} \mathbf{z}. \tag{12}$$

Therefore, solving for the GIC estimate is extremely quick; Eq. (12) requires simple matrix multiplication and $\mathbf{G}^{-1}$ is never explicitly inverted but solved using sparse matrix methods. Even then, the most computational taxing component, $\mathbf{G}^{-1}$, does not need to be found again unless the system topology changes. As with traditional SE, the proposed linear GIC estimator requires sufficient metering for redundancy and observability. Redundancy enables better estimates and the ability to filter out noisy or bad measurements. Observability is required to even obtain a solution. The results which follow demonstrate the estimate improvement with increased metering and future work will explore the minimum metering required for observability and meaningful results.

To validate this methodology, a synthetic GMD event will be applied to a test network. "Metered" measurements will be taken from the GIC solution and synthetic noise added. The underlying electric field state will be estimated and compared to the known driving electric field. Additionally, comparison between actual GIC neutral current values and values calculated from the estimate will be made. This will show the error that propagates in the presence of estimation error and the effect it might have on operating procedure usage. Overall, the proposed GIC estimator provides previously unavailable situational awareness to grid operators during a GMD that will enable improved response to and mitigation of GICs.

TABLE I
NEUTRAL CURRENTS FOR A GIC CALCULATION/ESTIMATION EXAMPLE

	Neutral Current (A)		
	T1	T2	T3
Actual	-297.8	129.4	168.4
Calculated	-271.9	106.4	167.2
Estimated	-299.9	130.8	171.3

C. A Basic Example

A simple example will show how the proposed method works and the system understanding improvement enabled by incorporating additional measurements. Consider the 6-bus system in Fig. 2 and assume there is an underlying spatially-varying electric field such that the left half of the system is experiencing a field with a particular magnitude while the right half experiences a different magnitude. The direction and size of the yellow arrows superimposed on the transmissions lines visualize the direction and magnitude of the resulting GIC flow. Assume there is one magnetometer installed on the right side of Fig. 2 from which the electric field in the region can be estimated, with decreasing certainty the further the value is applied from the magnetometer site. If no other measurements were available, someone who wanted an idea of GIC flows or reactive power losses in the area could calculate $\mathcal{I}_n$ using (7). The resulting neutral current calculation results are available in Table I, along with the actual values provided by a power flow simulation. The sign of the neutral current value indicates the direction of the current flow, with a positive value indicating amps flowing from the system into the neutral. A negative number indicates current flowing from the neutral into the system.

Because there is a different underlying field on the left side of the system, there is some error in the GIC calculation. This reiterates that with magnetometer measurements alone, neutral currents can be calculated, but data error is not able to be filtered out and higher granularity of states is not able to be achieved.

Now consider an available GIC neutral current measurement at Transformer 1 (T1) with a reading of -300 A. This transformer has the highest current in the system and is possibly monitored for this reason. Assuming this information can be aggregated with the electric field and topology information, GIC estimation is run to estimate the electric field of both the left and right sides of the system. It is assumed that the neutral current measurement is more heavily weighted than the electric field information, for which the weight is

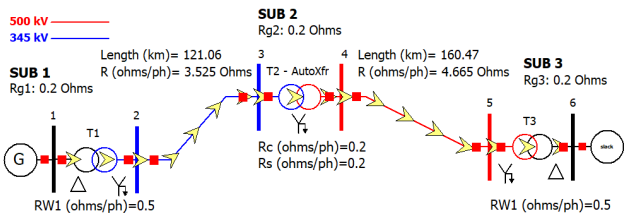

Fig. 2. Oneline of GIC estimation example with 6 buses and 3 substations

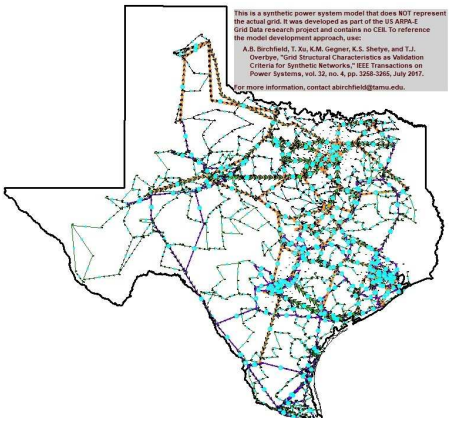

Fig. 3. Oneline of Texas 2000 synthetic case

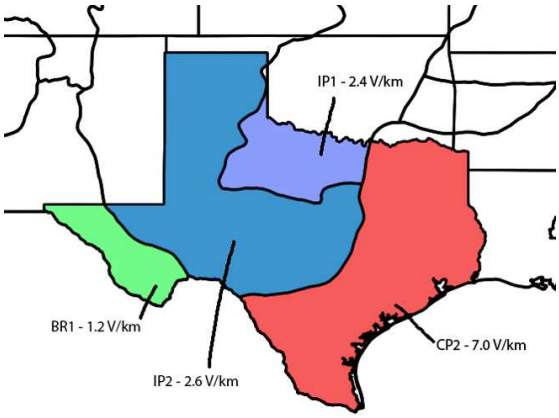

Fig. 4. Regional resistivity zones in the state of Texas (figure by Jennifer Gannon)

stronger on the right side than the left. This is consistent with the idea that confidence in electric field data is higher closer to the magnetometer data from which it is derived. The neutral current calculations resulting from the estimate are also shown in Table I. Note that with just the two measurements but without the GIC estimator, the current in T3 can be calculated and the measurement at T1 can override the wrong value calculated from the electric field measurement, but the current at T2 will have sizeable error without additional analysis. As seen in Table I, adding additional measurements or incorporating all available information into a tool like GIC estimation allows for a better understanding of $\mathcal{I}_n$ across the system. The next section provides more sophisticated analysis of the proposed methodology.

IV. RESULTS

A. Test Case

To demonstrate the proposed GIC estimation method, the process is tested on a 2000-bus synthetic system set on the footprint of the state of Texas [36]. The system has voltages ranging from 13.2 kV to 500 kV, nominal, and over 850 transformers, almost half of which are autotransformers. When electric field information is provided, GICs can be calculated in the system as the case, shown in Fig. 3, contains the

TABLE II
GIC ESTIMATION ERROR

	Electric Field (V/km)	Effective GICs (A/phase)
Mean Error	0.0605	0.2210
Max Error	0.1510	1.9911

necessary substation, transformer, and geographic data. The electric field is first assumed to be uniform within the 1D earth resistivity model regional zones shown in Fig. 4. In reality, the actual electric field variation across the region could be more complicated, which the example in Section IV-D addresses.

To generate artificially noisy measurements for use in the estimator, a subset of the GIC neutral current results are exported and random Gaussian noise is superimposed with varying variance. In practical applications, studies would need to be done and meter documentation referenced to deduce the error variances. In each of the following simulations, the installation locations of "measured" transformers are randomly chosen such that the pre-defined number of measurements is achieved with a balanced distribution of meters across zones. In these first studies, the number of such measurements spans from 0 to 100.

Six synthetic magnetic field meters are placed to emulate the number recently installed for the Texas magnetometer network. The location of the field meters is chosen to provide visibility in each of the regional resistivity zones and redundancy in the larger zones (by area). To generate synthetic electric field "measurements," the electric field information which was applied to the system to simulate a GMD is exported. Specifically it is saved at the locations of the synthetic magnetometers and random Gaussian noise is superimposed with varying variance. The actual process of determining geoelectric field from magnetic field measurements from magnetometers is covered in other literature and it is assumed that it can be carried out online. Since the underlying electric field state is known, the sensitivity of the GIC estimator to realistic conditions can be explored by comparing the estimated and actual states in different scenarios. The conditions covered here include varying of measurement noise and number of measurements.

The first result (Fig. 5) shows the potential situational awareness provided to grid operators from a particular instance of a limited set of 6 magnetometer and 16 transformer measurements, denoted by diamonds, using GIC estimation. Hence from 22 measurements the northward and eastward electric field components in the four resistivity zones (8 states) are estimated and the resulting GICs across the system calculated. Without comparable tools or metering all 800+ transformers in the system, it would not be known that 8 substations in the system have transformers with effective GICs over 50 A, denoted by red circles, or which transformers are at risk of having high GICs, denoted by yellow circles. Comparing these estimation results to the known actual values gives Table II. The resulting maximum and mean error (in V/km) are reasonable given noisy measurements, the effective GIC results which follow, and with respect to the magnitude of the true signal. Initial studies also show that the estimate error does not seem to be dependent on storm size or direction.

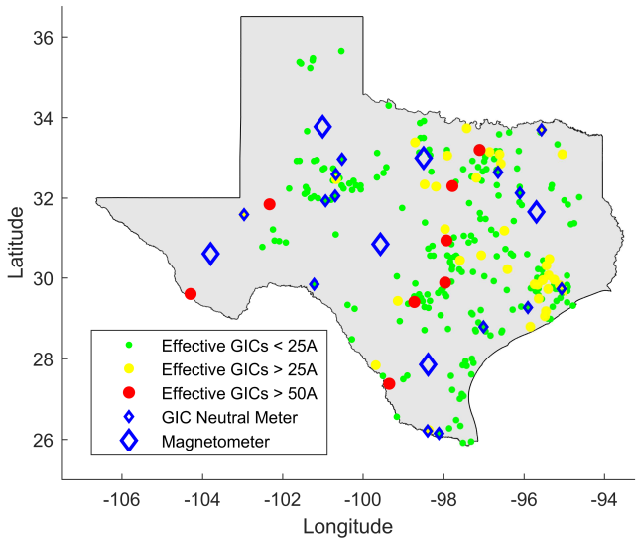

Fig. 5. Situational awareness for all transformers in the system (circles) from a limited set of measurements (diamonds) consisting of 6 magnetometers and 16 transformer neutral currents

B. Sensitivity to Electric Field Estimate Error

Determining the estimator's sensitivity to noise in the electric field input is valuable to understanding the practical usefulness of the tool under realistic conditions. Procuring these electric field inputs involves converting magnetic field data, likely from a magnetometer, into electric field data, using ground conductivity models. Error can be introduced both from noise in the magnetometer measurement and the conductivity transfer function. Here, the estimator's robustness to this variance is shown in Fig. 6. For a given storm represented by a uniform electric field (2 V/km east, 2 V/km north), the noise applied to the electric field is varied. Holding the number of electric field inputs, GIC neutral current measurements, and states to be estimated consistent with the scenario in Section IV-A, the resulting electric field estimate deviations are averaged over 1000 Monte Carlo simulations at each noise level. Fig. 6 shows that while extremely noisy or low confidence inputs may produce less-than desired results, generally the estimator provides useful results for grid operators. This motivates data quality standards for magnetometer installations and model accuracy standards for the online conversion from magnetic to electric field inputs.

C. Sensitivity to Measurement Availability

While GIC neutral current measurements are not currently very common, with developments like the proposed GIC estimator and increasing availability of magnetic field measurements, future installations are increasingly motivated. As in Section IV-A, the same states are estimated using the same electric field inputs. But in these scenarios, the number of available GIC measurements are varied. Fig. 7 shows the absolute value of the deviation between the estimated and

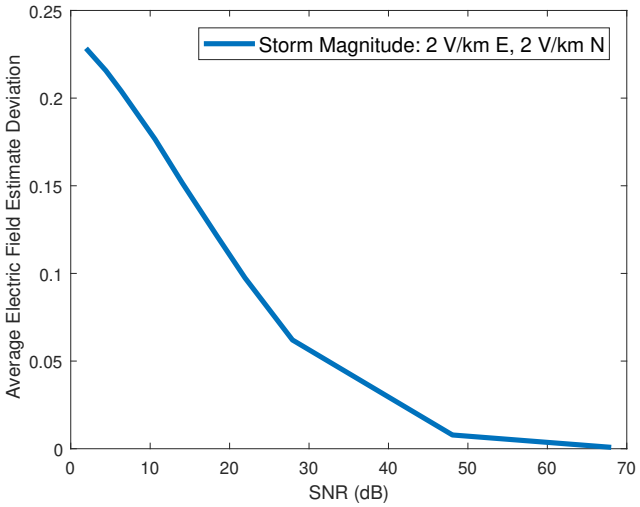

Fig. 6. Average electric field deviation (from 2 V/km) decreases as the noise of the electric field estimate (used as input) decreases

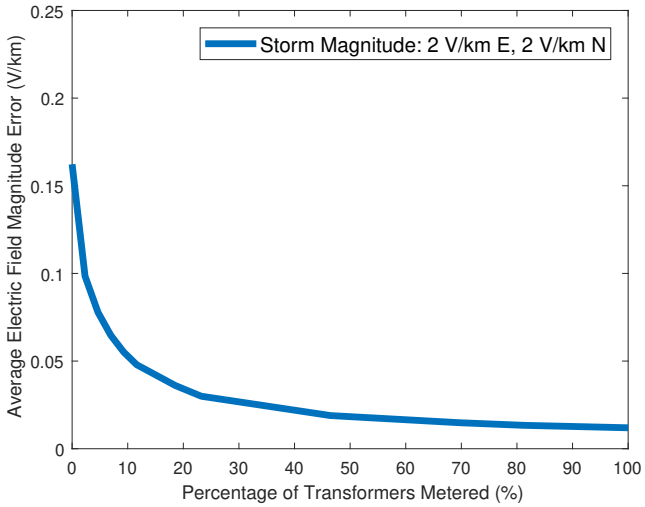

Fig. 7. Average electric field magnitude error decreases as the number of available GIC neutral measurements increases

actual electric field averaged over 1000 Monte Carlo simulations. It shows that as more GIC measurements are made available (out of a possible 861, for this particular scenario), the resulting electric field estimation is more accurate, which is to be expected as similar results are found in mainstream state estimation literature. Note that the greatest improvement in average electric field estimate deviation (denoted by the steeper slope) is found amongst the first 20% or so of measurements. While additional measurements do make a difference, for an already highly visible system it may not be cost effective to invest in additional meters for such a minuscule improvement at that point. It should be noted that these results would vary with differently defined electric field states, i.e. more measurements are required to estimate the electric field with finer granularity well. Continuing research on observability for GIC estimation methods will open interesting research questions as well as provide practical tools for electric utilities considering new metering installations.

D. Sensitivity to Granularity of Electric Field Zones

To recover and estimate smaller (more) zones requires additional metering to maintain observability. While the regional resistivity zones provide an idea of electric field variation due to geology, it is realistic to realize that the electric field may vary more than that, spatially speaking. With limited available magnetometer measurements, the usage of electric field "pseudomeasurements" may be utilized. To illustrate the estimation of more electric field zones on the same geographic footprint, an electric field with higher granularity of change is simulated. This electric field varies every 2 degrees latitude and longitude. In this example, the electric field magnitude and angle will be estimated for 20 distinct zones, where the zones are defined along the boundaries of a square grid. Along the perimeter of the system zones may be widened or lengthened by up to 0.25° to prevent the creation of an additional zone that would likely have limited measurement visibility due to its smaller area. These zones and their normalized electric field magnitude for a hypothetical snapshot in time are shown in Fig. 8; this is the actual state of the system. Given limited metering, pseudomeasurements are used in zones not directly metered. These values are determined by proximity to actual meters and influenced by the regional resistivity zones. Fig. 9 shows the pseudomeasurements and measurements used as input. The objective of the estimator is to recover the 20 zones/states as seen in Fig. 8.

The resulting absolute error for both electric field magnitude and angle estimates, averaged over 1000 Monte Carlo simulations, is shown in Fig. 10 for increasing penetration of transformer neutral metering. This is compared to the error of the noisy pseudomeasurements that have not been filtered by an estimation process or augmented with additional metering. Note that the error in Fig. 10 is greater than that in Fig. 7. This is due to the fact that, in this example, the underlying electric field is more spatially varying and thus more states are being estimated from roughly the same amount of data. As more meters are installed in a particular area, future research will provide more insight into the spatially varying properties of electric fields in that region and inform estimator design decisions with respect to estimation specificity.

Initial research on the trade-offs between estimating more or fewer zones shows that increasing the number of zones can better match the spatial variability of a realistic geomagnetic storm. This is dependent on there being sufficient metering to estimate all zones with reasonable accuracy. As seen in Fig. 11, for less than 30% of transformers (randomly) metered and the same 7 electric field inputs, estimating 12 zones provides better results than estimating 20 zones. This is due to the higher input needs of estimating more states.

E. Practical Considerations of Results

In practice, the estimated electric field states would be used to calculate GICs flowing through the system, which could be

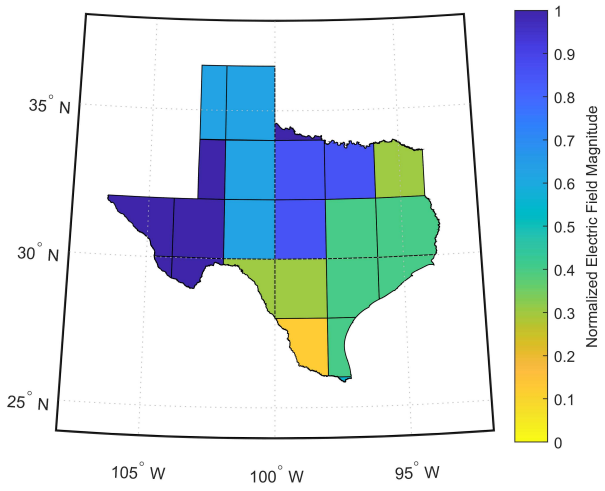

Fig. 8. An electric field with more spatial variation. In this example, the estimator will recover twenty zones, as opposed to just four in Fig. 4

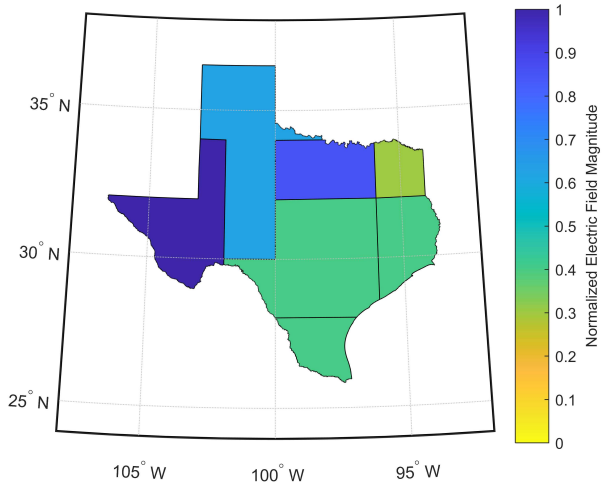

Fig. 9. Using 7 electric field inputs, this figure shows the electric field measurements and "pseudomeasurements" for zones without a magnetometer

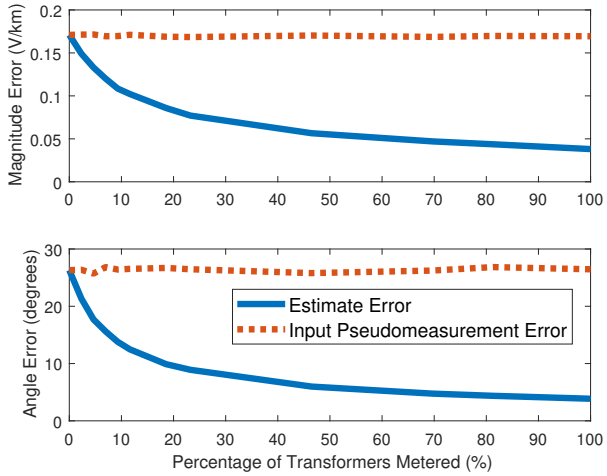

Fig. 10. Average absolute error for electric field magnitude and angle when estimating 20 zones with 7 magnetometers

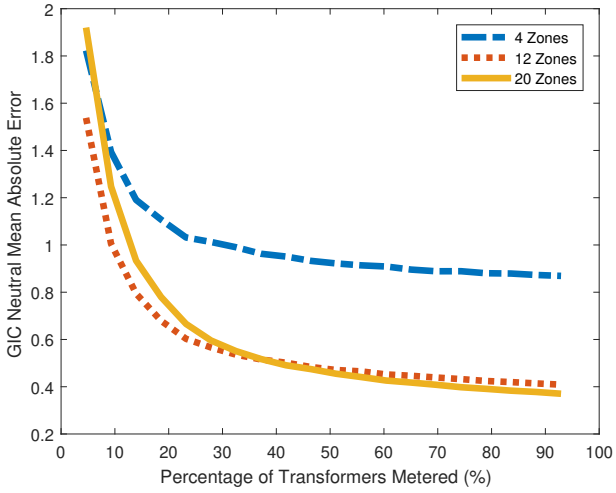

Fig. 11. GIC neutral mean absolute error for different number of zones with increasing transformer metering penetration

fed to some display providing situational awareness to grid operators. Effective GICs across the system are a powerful input to a variety of mitigation algorithms; hence an accurate estimate compared to merely considering the measured values could be the difference between taking the optimal action to mitigate GMD damage and taking actions that don't help or make the situation worse. It is prudent to have alarms tied to these values which would trigger for currents high enough to warrant closer consideration from grid operators. To validate the GIC estimation method under the realistic situation of high current alarms, a threshold of 50 A is set and the effective GICs across the system calculated from both the input "measurements" and the estimated states. Over 200 Monte Carlo simulations, the number of times that either technique produces a false alarm or fails to recognize a high current transformer is recorded and shown in Fig. 12. Without estimation, an average of two false positives and one missed alarm are encountered per simulation, regardless of the number of (random) available GIC measurements. With sufficient metering (about 15 GIC neutral meters) and estimation abilities, the potential of encountering an alarm error drops to less than once each per estimation run, and decreases with more measurements. On average, using GIC estimation does not create alarm errors that do not already exist as a result of using just the electric field inputs. This confirms that GIC estimation is a value-added process that is low risk in addition to low effort.

A common concern with SE algorithms is computational efficiency and run time. Because of the linear nature of GICs, this is not a worry for GIC estimation. In practice, the bigger barrier to generating estimates quickly lies in measurement latency. The estimation problem itself takes less than 0.0005 seconds using MATLAB on a PC with a processor Intel(R) Xeon(R) E5-1650 @ 3.6 GHz. The most computationally expensive part is the inverse in Eq. (12), which could become intensive as matrix size increases if no special matrix

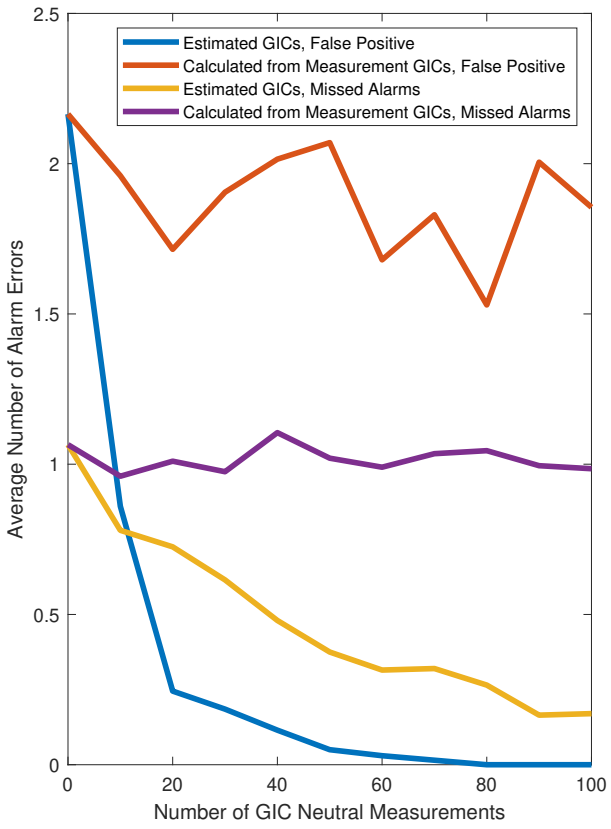

Fig. 12. Average number of false or missed alarms (50 A threshold) from measurements versus estimates, per simulation. There were 200 random simulations for each level of GIC neutral measurement availability.

properties are exploited. Fortunately the size of the matrix is two times the number of electric field areas, which would be naturally limited by available meters and the impracticability of estimating too many zones.

V. Summary and Future Work

To improve situational awareness during geomagnetic disturbances, a state estimation method was developed to provide an estimate of the state of GIC-related values in the system. It takes as input electric field and GIC neutral current data to return an estimate of the underlying electric field, from which GIC currents and resulting reactive power losses can be calculated. Because of GIC relationship linearity, the problem has an analytical solution. The methodology is demonstrated on a small scenario and on the synthetic Texas 2000-bus case. It is shown to be fast and accurate with sufficient metering. The solution alone can be provided to power grid operators to impart awareness and intuition during a GMD, or used as an input to a mitigation application or full ac state estimator to further inform operator response. Future work includes optimal placement of GIC meters as well as observability and bad data detection analysis. Additional study regarding more realistic models of the phenomena will also be undertaken, including improved measurement noise and error modeling, and estimator sensitivity to imperfect noise models. The proposed technique will be integrated into a simulated energy management system (EMS) environment for the real-time control and monitoring of the grid under GMDs.

References

[1] V. D. Albertson, J. M. Thorson, R. E. Clayton, and S. C. Tripathy, "Solar-Induced-Currents in Power Systems: Cause and Effects," *IEEE Transactions on Power Apparatus and Systems*, vol. PAS-92, no. 2, pp. 471–477, March 1973.

[2] "Effects of Geomagnetic Disturbances on the Bulk Power System," North American Electric Reliability Corporation (NERC), Tech. Rep., Feb 2012.

[3] V. D. Albertson, J. G. Kappenman, N. Mohan, and G. A. Skarbakka, "Load-Flow Studies in the Presence of Geomagnetically-Induced Currents," *IEEE Transactions on Power Apparatus and Systems*, vol. PAS-100, no. 2, pp. 594–607, Feb 1981.

[4] K. Shetye and T. J. Overbye, "Modeling and Analysis of GMD Effects on Power Systems: An overview of the impact on large-scale power systems," *IEEE Electrification Magazine*, vol. 3, no. 4, pp. 13–21, Dec 2015.

[5] "High-Impact, Low-Frequency Event Risk to the North American Bulk Power System," North American Electric Reliability Corporation (NERC), Tech. Rep., June 2010.

[6] "TPL-007-2 Transmission System Planned Performance for Geomagnetic Disturbance Events," North American Electric Reliability Corporation (NERC), Tech. Rep., Oct 2017.

[7] J. Berge, L. Martí, and R. K. Varma, "Modeling and mitigation of Geomagnetically Induced Currents on a realistic power system network," in *2011 IEEE Electrical Power and Energy Conference*, Oct 2011, pp. 485–490.

[8] D. H. Boteler and R. J. Pirjola, "Modeling geomagnetically induced currents," *Space Weather*, vol. 15, no. 1, pp. 258–276, Jan 2017.

[9] T. J. Overbye, K. S. Shetye, T. R. Hutchins, Q. Qiu, and J. D. Weber, "Power Grid Sensitivity Analysis of Geomagnetically Induced Currents," *IEEE Transactions on Power Systems*, vol. 28, no. 4, pp. 4821–4828, Nov 2013.

[10] M. Kazerooni, H. Zhu, T. J. Overbye, and D. A. Wojtczak, "Transmission System Geomagnetically Induced Current Model Validation," *IEEE Transactions on Power Systems*, vol. 32, no. 3, pp. 2183–2192, May 2017.

[11] K. S. Shetye, T. J. Overbye, Q. Qiu, and J. Fleeman, "Geomagnetic disturbance modeling results for the AEP system: A case study," in *2013 IEEE Power & Energy Society General Meeting*, July 2013, pp. 1–5.

[12] K. Zheng, D. Boteler, R. J. Pirjola, L. Liu, R. Becker, L. Martí, S. Boutilier, and S. Guillon, "Effects of System Characteristics on Geomagnetically Induced Currents," *IEEE Transactions on Power Delivery*, vol. 29, no. 2, pp. 890–898, April 2014.

[13] C. Basu, M. Padmanaban, S. Guillon, M. de Montigny, and I. Kamwa, "Combining multiple sources of data for situational awareness of geomagnetic disturbances," in *2015 IEEE Power & Energy Society General Meeting*, July 2015, pp. 1–5.

[14] C. Klauber and H. Zhu, "Power network topology control for mitigating the effects of geomagnetically induced currents," in *2016 50th Asilomar Conference on Signals, Systems and Computers*, Nov 2016, pp. 313–317.

[15] M. Kazerooni, H. Zhu, and T. J. Overbye, "Mitigation of Geomagnetically Induced Currents Using Corrective Line Switching," *IEEE Transactions on Power Systems*, vol. 33, no. 3, pp. 2563–2571, May 2018.

[16] H. Zhu and T. J. Overbye, "Blocking device placement for mitigating the effects of geomagnetically induced currents," in *2016 IEEE Power & Energy Society General Meeting*, July 2016, pp. 1–1.

[17] L. Martí, A. Rezaei-Zare, and A. Yan, "Modelling considerations for the Hydro One real-time GMD management system," in *2013 IEEE Power & Energy Society General Meeting*, July 2013, pp. 1–6.

[18] A. Yan, D. Zhou, and L. Martí, "Analysis of Geomagnetically Induced Currents," in *2013 IEEE Power & Energy Society General Meeting*, July 2013, pp. 1–6.

[19] A. Abur and A. Gómez, *Power System State Estimation-Theory and Implementations*. Marcel Dekker, Inc., 2004.

[20] A. Monticelli, "Electric power system state estimation," *Proceedings of the IEEE*, vol. 88, no. 2, pp. 262–282, Feb 2000.

[21] F. C. Schweppe and J. Wildes, "Power System Static-State Estimation, Part I: Exact Model," *IEEE Transactions on Power Apparatus and Systems*, vol. PAS-89, no. 1, pp. 120–125, Jan 1970.
[22] C. Klauber, G. P. Juvekar, K. Davis, T. J. Overbye, and K. Shetye, "The Potential for a GIC-inclusive State Estimator," in *2018 North American Power Symposium (NAPS)*, Sep. 2018, pp. 1–6.
[23] M. Lu, S. D. Eksioglu, S. J. Mason, R. Bent, and H. Nagarajan, "Distributionally robust optimization for a resilient transmission grid during geomagnetic disturbances," *arXiv, 1906.04139*, 2019.
[24] L. Gong, Y. Fu, M. Shahidehpour, and Z. Li, "A Parallel Solution for the Resilient Operation of Power Systems in Geomagnetic Storms," *IEEE Transactions on Smart Grid*, pp. 1–1, 2019.
[25] D. H. Boteler, L. Trichtchenko, R. Pirjola, J. Parmelee, S. Souksaly, A. Foss, and L. Martí, "Real-Time Simulation of Geomagnetically Induced Currents," in *2007 7th International Symposium on Electromagnetic Compatibility and Electromagnetic Ecology*, June 2007, pp. 261–264.
[26] S. Watari, "Estimation of geomagnetically induced currents based on the measurement data of a transformer in a Japanese power network and geoelectric field observations," *Earth, Planets and Space*, vol. 67, no. 1, May 2015.
[27] M. Kazerooni, H. Zhu, K. Shetye, and T. J. Overbye, "Estimation of geoelectric field for validating geomagnetic disturbance modeling," in *2013 IEEE Power and Energy Conference at Illinois (PECI)*, Feb 2013, pp. 218–224.
[28] D. H. Boteler and R. J. Pirjola, "Modelling geomagnetically induced currents produced by realistic and uniform electric fields," *IEEE Transactions on Power Delivery*, vol. 13, no. 4, pp. 1303–1308, Oct 1998.
[29] S. Cuttler, J. Love, and A. Swidinsky, "Geoelectric hazard assessment: the differences of geoelectric responses during magnetic storms within common physiographic zones," *Earth, Planets, and Space*, 2018.
[30] K. D. Jones, J. S. Thorp, and R. M. Gardner, "Three-phase linear state estimation using Phasor Measurements," in *2013 IEEE Power & Energy Society General Meeting*, July 2013, pp. 1–5.
[31] L. Zhang, A. Bose, A. Jampala, V. Madani, and J. Giri, "Design, Testing, and Implementation of a Linear State Estimator in a Real Power System," *IEEE Transactions on Smart Grid*, vol. 8, no. 4, pp. 1782–1789, July 2017.
[32] T. Yang, H. Sun, and A. Bose, "Transition to a Two-Level Linear State Estimator—Part II: Algorithm," *IEEE Transactions on Power Systems*, vol. 26, no. 1, pp. 54–62, Feb 2011.
[33] Boteler, David, "Methodology for simulation of geomagnetically induced currents in power systems," *J. Space Weather Space Clim.*, vol. 4, p. A21, 2014.
[34] J. L. Gannon, A. B. Birchfield, K. S. Shetye, and T. J. Overbye, "A Comparison of Peak Electric Fields and GICs in the Pacific Northwest Using 1-D and 3-D Conductivity," *Space Weather*, vol. 15, no. 11, pp. 1535–1547, 2017.
[35] United States Geological Survey, "Regional conductivity maps." [Online]. Available: https://geomag.usgs.gov/conductivity/
[36] "Texas 2000-bus system." [Online]. Available: https://electricgrids.engr.tamu.edu/electric-grid-test-cases

Cecilia Klauber (S'12) received the B.S. degree in electrical engineering from Baylor University, Waco, TX, USA in 2014 and the M.S. degree in electrical engineering from the University of Illinois at Urbana-Champaign, Champaign, IL, USA in 2016. She is currently a Ph.D candidate in electrical engineering at Texas A&M University, College Station, TX, USA.

Komal Shetye (S'10-M'11-SM'18) received the B. Tech and MSEE degrees in electrical engineering from the University of Mumbai, India and the University of Illinois at Urbana-Champaign, IL, USA, in 2009 and 2011, respectively. She is currently an Associate Research Engineer with the Texas Engineering Experiment Station (TEES) and the Department of Electrical Engineering, Texas A&M University, College Station, TX, USA.

Thomas J. Overbye (S'87-M'92-SM'96-F'05) received B.S., M.S., and Ph.D. degrees in electrical engineering from the University of Wisconsin Madison, Madison, WI, USA. He is currently with Texas A&M University where he is a Professor and holder of the Erle Nye '59 Chair for Engineering Excellence.

Katherine R. Davis (S'05-M'12-SM'18) received the B.S. degree from the University of Texas at Austin, Austin, TX, USA, in 2007, and the M.S. and Ph.D. degrees from the University of Illinois at Urbana-Champaign (UIUC), Urbana, IL, USA, in 2009 and 2011, respectively, all in electrical engineering. She is currently an Assistant Professor in electrical and computer engineering with Texas A&M University, College Station, TX, USA.